

Parametrization of Microbial Survival Models under UVC Exposure

Aikaterini A. Tsantari, Konstantinos K. Delibasis, Harilaos G. Sandalidis, and Nestor D Chatzidiamantis, *Member, IEEE*

Abstract

This study aims to identify and parameterize the optimal survival curves for 33 fundamental microorganisms subject to UVC exposure through experimental measurements. We compile published data on UVC doses and corresponding survival fractions for these microorganisms to estimate parameters for four prominent survival models: Single-target (ST), Multi-target (MT), Linear Quadratic (LQ), and Two-Stage Decay (TSD). The best-fitting model for each microorganism is determined by selecting the one with the lowest mean squared error (MSE) compared to the experimental data. Our analysis indicates that the MT model is the most frequently appropriate, accurately fitting 21 of the 33 microorganisms. The TSD model is the best fit for only three, while the LQ model, though occasionally suitable at lower doses, is often excluded due to unreliable performance at higher doses. The assessed models, particularly the MT model, demonstrate strong predictive capabilities for UVC surface sterilization of microorganisms. However, caution is warranted with the LQ model at higher doses due to its potential limitations.

Index Terms

Microorganisms, parametrization, survival models, UVC exposure

I. INTRODUCTION

Ultraviolet (UV) radiation covers the wavelength range of 100 to 400 nm and is divided into four subcategories: UVA (315-400 nm), UVB (280-315 nm), and UVC (100-280 nm) [1]. UVC,

Aikaterini A. Tsantari and Nestor D. Chatzidiamantis are with the Department of Electrical and Computer Engineering, Aristotle University of Thessaloniki, 54124 Thessaloniki, Greece e-mails{ktsantari, nestoras}@auth.gr.

Konstantinos K. Delibasis and Harilaos G. Sandalidis are with the Department of Computer Science and Biomedical Informatics, University of Thessaly, Papasiopoulou 2-4, 35 131, Lamia, Greece. e-mails{kdelimpasis, sandalidis}@uth.gr.

in particular, is harmful to humans, causing skin and eye damage as well as cancer [2]. Specific wavelengths within the UV spectrum can sterilize air and surfaces. This application, known as ultraviolet germicidal irradiation (UVGI), primarily utilizes UVB and UVC wavelengths (200-320 nm) [3].

UVC radiation is absorbed by proteins, RNA, and DNA, resulting in cellular damage. This absorption induces mutations, often leading to the inactivation or death of microorganisms. Microbial inactivation refers to losing the ability to reproduce or multiply without necessarily damaging its genetic material, rendering the organism non-pathogenic [4]. During partial dormancy, the microbe can reactivate, initiating multiplication after UVC exposure, utilizing various cellular mechanisms [5]. Microbial death occurs upon receiving a sufficient dose of radiation, termed the lethal dose. Although the inactivation mechanism applies to all microorganisms, including fungi, bacteria, or viruses, their sensitivity to UV exposure may vary significantly. Consequently, the lethal dose or exposure time can vary between microorganisms [6]. Hence, the effectiveness of UVC radiation in disinfecting a microorganism depends not only on the exposure time but also on the specific genomic regions affected [7].

The survival of microorganisms on surfaces is influenced by various factors, including the microorganism's type, structure, and chemical composition. Consequently, microorganisms within the same family, such as Sars-CoV-1 and Sars-CoV-2, exhibit similar lethal doses [7], [8]. Environmental conditions such as temperature, relative humidity, and surface material also play significant roles [9]–[11], with relative humidity having different effects on viruses and bacteria, while its influence on fungi is minimal [3]. The characteristics of the surface, including its color, texture, and density, are crucial in determining the absorption or reflection of photons, thereby affecting the amount of radiation it absorbs [2], [11]. Moreover, the correct arrangement of light sources in a room is paramount in practical settings [12]. Finally, it is critical to recognize that microorganism distribution within a space is dynamic and subject to variation [13].

For some microorganisms, different doses of UV radiation were found to cause different reductions in their cell colonies. A survival model is a mathematical expression of survival versus radiation dose. Given a parameterized survival model for a microorganism, it is possible to calculate its survival fraction (equivalently, the reduction) for any radiation dose within a specific range. The curve for this model is usually plotted on a logarithmic scale for the y-axis. The shape of the curve varies depending on the mathematical formula chosen to express it [3].

Overall, survival models for microorganisms under UVC radiation are indispensable tools for

enhancing the safety, efficiency, and sustainability of disinfection methods. In research, they help understand UV damage mechanisms and foster innovation in UVC technology. Additionally, they aid in designing safety protocols for UVC exposure and devising decontamination strategies in emergencies, making them essential across various fields and applications.

Inspired by these benefits, the present study comprehensively reviews existing literature and experimental data on UVC doses and the corresponding survival fractions for some critical microorganisms. We then examine four commonly used cell survival models: the Single-target (ST), the Multi-target (MT), the Linear-Quadratic (LQ), and the Two-stage decay (TSD) model, and estimate the parameters of each model for 33 different microorganisms. Finally, we determine the best-fitting model based on the mean squared error (MSE) relative to the experimental data. We believe that the fitting model and its parameters hold potential for diverse applications in surface disinfection pertinent to public health and infectious disease control. To our knowledge, such an analysis remains unexplored in the academic medical literature. Thus, this study aims to address this gap that has not been sufficiently explored in prior research.

II. UVC DISINFECTION STUDIES

Various investigations explore the inactivation of microorganisms using UVC radiation. Some studies involve practical measurements in real-world settings, such as [11], [12], [14]–[16], while others focus on experimental measurements conducted in laboratory conditions, for instance [6], [17]–[20]. All these studies center around assessing the survival of microorganisms, quantified on a logarithmic scale based on 10. For example, a 1log reduction corresponds to a 90% reduction (0.1 survival) from the initial microbial population [21]. The reduction levels commonly observed are detailed in Table I. Measurement involves counting the colony-forming units (CFU) initially present and those remaining after exposure.

Drawing from multiple published studies, Table II summarizes the reduction observed in some critical microorganisms following exposure to a specific dose of UVC radiation under specified distances and durations, together with the corresponding references. Some surveys had similar tables prepared; thus, not all of their information was displayed again. Finally, some studies do not report the distance from the source or the operational time; hence, only a dash is noted.

The most prevalent wavelengths of UV radiation for microorganism inactivation are 222 nm and 254 nm. Recent studies [17], [18] suggest that 222 nm radiation is less harmful to humans because it penetrates only superficially and does not breach the cell walls of skin cells or the

TABLE I
LOGARITHMIC MEASUREMENT OF MICROORGANISM'S COLONY REDUCTION.

Surviving Fraction	Log Reduction	Percentage Reduction	Survival Percentage
0.1	1 log	90%	10%
0.01	2 log	99%	1%
0.001	3 log	99.90%	0.10%
0.0001	4 log	99.99%	0.01%
0.00001	5 log	99.999%	0.001%
0.000001	6 log	99.9999%	0.0001%

eye's outer layer. Nevertheless, it retains its sterilizing efficacy, making it advisable for use in public places [18]. Conversely, wavelengths less than 240 nm (in the far-UVC band) generate ozone through the interaction of photons with oxygen molecules, leading to harmful effects and significant air pollution [2], [5], [7].

As depicted in Table II and corroborated by [7], coronaviruses exhibit higher UV radiation resistance than *Escherichia coli* bacteria, necessitating significantly greater radiation doses for inactivation. Moreover, [17] asserts that 222 nm is particularly effective against bacterial endospores, whereas 254 nm yields superior results for fungal spores and hyphae.

Similar tables have been documented in the literature based on laboratory measurements or experimental assessments conducted in real-world settings [7], [11], [15], [19]. Specifically, [11] and [15] provide measurements for various common microorganisms including *Bacillus subtilis* ATCC6633, *Campylobacter jejuni* ATCC43429, *Citrobacter diversus*, *Escherichia coli*, *Klebsiella pneumoniae*, *Legionella pneumophila* ATCC33152, *Shigella dysenteriae*, *Shigella sonnei* ATCC9290, *Staphylococcus aureus* ATCC25923, and *Streptococcus faecalis* ATCC29212. Furthermore, data regarding air disinfection of microorganisms and measurements involving animal cells are available in [19]. While air decontamination shares similarities with surface decontamination, both differ significantly from water decontamination [2], [22].

It is notable to reference the findings of [15], which explore the disinfection of face masks using the DIALux simulator for theoretical sterilization studies. The research demonstrates the time required to disinfect masks with specific radiation doses and discusses that the region nearest to the source does not always receive the highest dose and, consequently, the most effective

TABLE II
MICROORGANISM DISINFECTION STUDIES.

*: SPECIFIC TABLES PROVIDE DETAILED INFORMATION ON THE SURVIVAL OF PARTICULAR MICROORGANISMS.

Microorganism	UV Source	Dose	Log Reduction	Time of Exposure	Distance from Source	Reference
Coronaviruses	UV	3.7 mJ/cm ²	1log	-	-	[20]
Sars-CoV	240-280 nm	1445 mJ/m ²	2log	6 min	3 cm	[14]
Sars-CoV	254 nm	4016 μ W/cm ²	8log	2 h	3 cm	[22]
Sars-CoV-1	15 W UVC	36144 J/m ²	5log	20 min	0.15 m	[8]
Sars-CoV-2	254 nm	30 mJ/cm ²	full inactivation	-	various	[12]
Coronaviruses	UVA, UVC	*	*	-	-	[19]*
Coronaviruses	UVC	*	*	-	-	[7]*
Rotavirus	254 nm	25 mJ/cm ²	3log	-	-	[20]
Adenovirus	254 nm	140 mJ/cm ²	3log	-	-	[20]
Vaccinia	15 W 254 nm	90 J/m ²	3log	0-30 s	0.3 m	[23]
Lassa	15 W 254 nm	90 J/m ²	97%	0-30 s	0.3 m	[23]
Ebola	15 W 254 nm	90 J/m ²	4log	0-30 s	0.3 m	[23]
Influenza A	222 or 254 nm	6 mJ/cm ²	non detectable	-	-	[17]
Spores and Bacteria	254 nm	*	*	-	-	[11]*
Viruses, Spores, Bacteria, Yeasts	253.7 nm	*	4log	-	-	[16]*
Clostridium difficile spore	254 nm	38.5 mJ/cm ²	4log	-	-	[12]
Staphylococcus aureus (MRSA)	222 nm	6 mJ/cm ²	4log	-	-	[17]
	254 nm	12 mJ/cm ²	non detectable	-	-	[17]
Pseudomonas aeruginosa	222 nm	6 or 24 mJ/cm ²	2log or 3log	-	-	[17]
	254 nm	6 mJ/cm ²	non detectable	-	-	[17]
Escherichia coli	222 nm	6 or 24 mJ/cm ²	2log or 3log	-	-	[17]
	254 nm	6 mJ/cm ²	non detectable	-	-	[17]
Salmonella enterica s.en.s	222 nm	12 or 36 mJ/cm ²	2log or non detectable	-	-	[17]
	254 nm	24 mJ/cm ²	3log	-	-	[17]
Campylobacter jejuni	222 or 254 nm	6 mJ/cm ²	non detectable	-	-	[17]
Clostridium sporogenes	222 nm	36 mJ/cm ²	non detectable	-	-	[17]
	254 nm	72 mJ/cm ²	non detectable	-	-	[17]
Clostridiodes difficile	222 nm	50 mJ/cm ²	non detectable	-	-	[17]
	254 nm	30 mJ/m ²	non detectable	-	-	[17]
Candida albicans	222 or 254 nm	72 mJ/cm ²	non detectable	-	-	[17]
Aspergillus niger	222 nm	500 mJ/m ²	non detectable	-	-	[17]
	254 nm	250 mJ/cm ²	non detectable	-	-	[17]
Trichophyton rubrum	222 nm	72 mJ/cm ²	non detectable	-	-	[17]
	254 nm	36 mJ/cm ²	non detectable	-	-	[17]

disinfection. Material properties, including reflection and scattering coefficients, can influence this phenomenon.

III. SURVIVAL MODELS

Mathematical modeling of microorganism survival often assumes that each microorganism has one or more targets that must be hit for its complete inactivation, leading to the development of

corresponding models such as the ST, MT, and LQ. A target is a sensitive region in the DNA molecule whose exposure to UV radiation can cause cell death [24]. The simplest survival model is the ST model with one target. Its mathematical expression is given by

$$S = e^{-D/D_0}, \quad (1)$$

where D is the dose variable, and D_0 is the dose required to reduce cell survival by a factor of e^{-1} . Radiative emissions are assumed to be Poisson-distributed [25]. Survival curves are commonly plotted in a semi-logarithm graph. Substituting $\alpha = -1/D_0 < 0$, (1) transforms to

$$S = e^{\alpha D}, \quad (2)$$

where the coefficient α takes different values for each microorganism. The MT model [3], [24], [26] is given by the mathematical expression

$$S = 1 - (1 - e^{-D/D_0})^\beta, \quad (3)$$

where β represents the number of targets per cell that must be hit to deactivate the cell [24], [26]. This model is particularly applicable to microorganisms exposed to high and low linear energy transfer (LET) radiation, such as UVC photons, depending on the value of β [24]. In the latter case, where $\beta > 1$, a shoulder appears in the region of low doses in the survival curve [25]. For this model, the coefficient α is again defined as the quotient $-1/D_0$. Therefore, (3) is written as

$$S = 1 - (1 - e^{\alpha D})^\beta. \quad (4)$$

The next model analyzed in this work is the LQ, which is expressed by:

$$S = e^{-\alpha D - \beta D^2}. \quad (5)$$

This curve also exhibits a non-linearity, which is affected by the ratio α/β of the coefficients. Thus, the LQ model could be considered a combination of the previous two. According to [25], the LQ model often has a somewhat similar form to the MT model—especially for a few experimental points, which is also confirmed in the curves below for various microorganisms.

However, some microorganisms display a distinct survival pattern: while a large portion is vulnerable to radiation, a small fraction is more resistant. This results in an initial rapid population

decline, followed by a slower decrease. In such cases, the abovementioned models do not align with experimental observations. A more appropriate model is the TSD [3]

$$S = f_1 e^{-k_1 D} + f_2 e^{-k_2 D}, \quad (6)$$

where k_1 and k_2 are the two reciprocal equivalents of D_0 in the other models, and the parameters f_1 and f_2 are positive numbers in $[0, 1]$, generalizing the standard TSD model in which $f_2 = 1 - f_1$, with f_1 being the sensitive fraction of the population.

IV. SURVIVAL MODEL PARAMETRIZATION

The survival models can be parameterized for various microorganisms using experimental measurements specific to each type [7], [11]. In [11], such measurements are gathered from the literature and experimentally validated in a hospital room at different distances from the source, both in areas with and without a direct line-of-sight (LOS) to the source. Similarly, a study on SARS-CoV-2 is conducted at 254 nm, one of the preferred wavelengths for sterilization [7].

In particular, for the ST model, the i -th experimental measurement $(D_i, S_i), i = 1, \dots, N$ of a microorganism should satisfy the model equation. By applying logarithmic transformations to these expressions and employing table-based formalism, we derive the following equation:

$$\mathbf{D}\alpha = \mathbf{S}_L, \quad (7)$$

where $\mathbf{D} = [D_1, \dots, D_N]^T$ is the column matrix of the doses of the points, $\mathbf{S}_L = -[\ln S_1, \dots, \ln S_N]^T$ is the column matrix of the corresponding logarithmic survivals, and α is the unknown model parameter.

Eq. (7) is solved for α by linear least squares minimization, equivalent to multiplying from the left with \mathbf{D}^T . The final calculation formula for α is shown below:

$$\alpha = \frac{\sum_{i=1}^N D_i S_{L_i}}{\sum_{i=1}^N D_i^2}, \quad (8)$$

where N is the total number of experimental data for each microorganism.

The parameters α and β are estimated as follows for the MT model. First, we will prove the following Lemma.

Lemma 1. *The gradient of the logarithm of the survival for the MT model for large values of dose D is independent of the number of targets per cell, β .*

Proof. By differentiating the logarithm of S with respect to D in (4), we obtain

$$\frac{d}{dD} \ln S = \frac{\beta(1 - e^{-D/D_0})^\beta}{D_0 (e^{-D/D_0} - 1) \left(1 - (1 - e^{-D/D_0})^\beta\right)}. \quad (9)$$

It is easy to show that

$$\lim_{D \rightarrow \infty} \frac{d(\ln S)}{dD} = -\frac{1}{D_0} = a, \quad (10)$$

which concludes the proof. \square

By using the above Lemma, we can employ linear regression to the experimental data points

$$\log S_i = \alpha D_i + c, \quad (11)$$

in order to estimate the gradient of $\log S$, $\alpha = -\frac{1}{D_0}$, provided that the corresponding doses lie beyond the shoulder of the curve. Finally, the number of targets per cell is obtained by $\beta = e^c$ [24].

Additionally, for the LQ model, the constants α and β of (5) need to be calculated for each microorganism by minimizing the error with respect to the N experimental measurements (D_i, S_i) . By applying (5) to each experimental measurement and taking the logarithm, we can rewrite the linear equations (with respect to α, β) in matrix form

$$\mathbf{D} \cdot \mathbf{P} = \mathbf{S}_L, \quad (12)$$

where $\mathbf{P} = [\alpha, \beta]^T$, \mathbf{D} is the 2-columned matrix of the doses of the points, where each line is (D_i, D_i^2) , and \mathbf{S}_L is the column matrix of the negative logarithmic survivals:

$$\mathbf{D} = \begin{bmatrix} D_1 & D_1^2 \\ D_2 & D_2^2 \\ \vdots & \vdots \\ D_N & D_N^2 \end{bmatrix}, \quad \mathbf{S}_L = - \begin{bmatrix} \ln S_1 \\ \ln S_2 \\ \vdots \\ \ln S_N \end{bmatrix}. \quad (13)$$

A simple linear regression is performed using the least squares method to solve this system and estimate the final values of the parameters α and β .

Finally, for the TSD model, four parameters, f_1 , k_1 , f_2 , and k_2 , need to be estimated. To this end, the least squares method is used with the iterative Gauss-Newton algorithm.

V. RESULTS

The above methodology was applied to the experimental measurements of 33 microorganisms. To select the optimal survival model for each microorganism, the mean squared error (MSE) between measurements and model prediction was calculated for each model. The model that achieved the minimal MSE was selected as the appropriate one for each specific microorganism.

In view of the above, Table III presents the selected survival model in terms of the achieved MSE for each microorganism and the estimated parameter values. Moreover, Fig. 1 depicts ST, MT, and LQ model curves for three microorganisms. It is noteworthy that $-x \log_{10}$ refers to 10^{-x} survival.

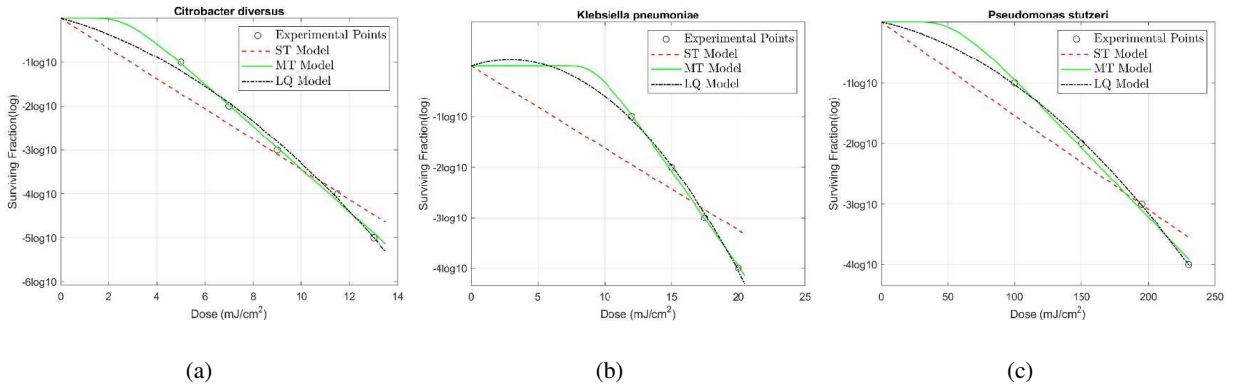


Fig. 1. Survival models for three microorganisms.

In certain microorganisms, such as SARS-CoV-2, the LQ model achieves the lowest MSE. However, this model is inadequate for larger doses because it corresponds to a quadratic polynomial on the logarithmic scale. This polynomial may exhibit an ascending trend with increasing doses in specific scenarios. It is easy to verify that the extremum point of the LQ model appears at:

$$l = -\frac{\alpha}{2\beta} \quad (14)$$

For microorganisms where $l > 0$ and $l < D_{\max}$, with D_{\max} being the maximum dose considered under realistic disinfection scenarios, the model survival curve exhibits the aforementioned ascending behavior. Thus, the LQ model is discarded in such cases. For the LQ model to be concave and acceptable, it must satisfy $l < 0$ and $-\beta < 0$ or equivalently $\beta > 0$. Therefore, the next best model (in terms of MSE) is selected for these microorganisms.

In Table III, these microorganisms are marked with the footnote symbol: "1". Figure 2 illustrates that the LQ model for SARS-CoV-2 seems more suitable for doses below 40 mJ/cm^2 ;

TABLE III

FINAL MODEL SELECTION AND CORRESPONDING PARAMETERS FOR EACH MICROORGANISM.

¹: THE SELECTED MODEL FOR THESE MICROORGANISMS DOES NOT YIELD THE MINIMUM MSE.

*: THE TSD MODEL BEST FITS THIS MICROORGANISM, MINIMIZING THE MSE; FURTHER DETAILS ARE AVAILABLE IN

TABLE IV.

Microorganism	MMSE	Survival Model	α	β
Bacillus subtilis ATCC6633 ¹	2	MT	-0.1202	-0.1953
Bacillus subtilis WN626 ¹	0.3338	MT	-4.3699	-0.7311
Campylobacter jejuni ATCC 43429	1.7647	LQ	1.0734	0.1581
Citrobacter diversus	0.2233	MT	-1.1186	3.2711
Citrobacter freundii	0.0004986	MT	-0.5756	0.5756
Escherichia coli ATCC 11229	0.9507	MT	-1.7403	9.4513
Escherichia coli ATCC 11303	0.8724	MT	-1.0368	1.7909
Escherichia coli ATCC 25922	2.1554	MT	-2.7631	13.355
Escherichia coli K12 IFO3301	0.0097	LQ	1.0288	0.0013
Escherichia coli O157:H7 ATCC 43894	0.048	MT	-1.7168	0.2342
Escherichia coli O157:H7 CCUG 29193	0.3507	MT	-2.0115	4.6532
Escherichia coli O157:H7 CCUG 29197	2.285	LQ	0.2944	0.31
Escherichia coli O157:H7 CCUG 29199	1.1096	LQ	2.9215	4.7497
Escherichia coli O157:H7*	0.0032	TSD	-	-
Klebsiella pneumoniae	0.0474	MT	-0.867	8.2247
Legionella pneumophila ATCC 43660	0.1398	MT	-1.1015	0.9628
Legionella pneumophila ATCC33152A	0.0043	MT	-1.193	-0.0363
Legionella pneumophila ATCC33152B	4.14×10^{-30}	ST	-1.4391	-
Pseudomonas stutzeri	0.0178	LQ	0.0112	0.0001
Salmonella e.s. E.s. Typhimurium ¹	0.0022	MT	-0.1919	-2.3026
Salmonella spp.*	0.0028	TSD	-	-
Salmonella typhi ATCC 19430	0.456	LQ	0.9444	0.0204
Salmonella typhi ATCC 6539	0.0362	MT	-1.5762	1.8876
Salmonella typhimurium hf ¹	1.7651	MT	-0.9528	-1.1116
Salmonella typhimurium	0.7957	LQ	0.0396	0.000021423
Shigella dysenteriae ATCC29027*	0.492	TSD	-	-
Shigella sonnei ATCC9290	0.005	MT	-1.3869	2.1489
Staphylococcus aureus ATCC25923	2.2527	MT	-1.0236	0.9481
Streptococcus faecalis ATCC29212 ¹	0.6274	MT	-1.5064	7.9895
Streptococcus faecalis se	2.7061	MT	-1.4107	4.6598
Vibrio natriegens	0.1369	LQ	0.0509	0.0002
Yersinia ruckeri ¹	0.8602	MT	-1.7105	-1.0526
Sars-CoV-2 ¹	0.8296	MT	-0.2911	-2.4176

nevertheless, depending solely on this model leads to inaccurate results for higher exposures.

Thus, the MH model is selected, as indicated in the last line of Table III.

Finally, the most prevalent model is the MT model, identified in 21 of the 33 microorganisms

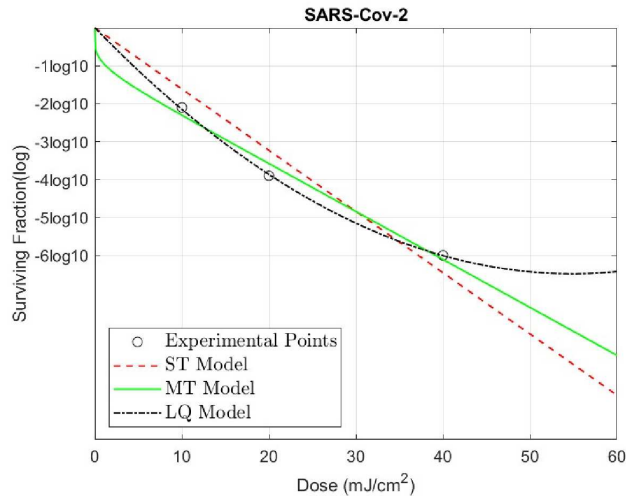


Fig. 2. Surviving models for SARS-CoV-2.

considered in this study. Three microorganisms exhibit measurements better modeled by the TSD model. However, this model is unsuitable for the rest of the microorganisms. These three microorganisms are annotated with the footnote symbol: ”*” in Table III, while the corresponding parameters and the achieved MSE for the best TSD model are provided in Table IV. Figure 3 illustrates the survival models with their optimal parameterization for *Escherichia coli* O157, *Salmonella* spp., and *Shigella dysenteriae* ATCC29027, confirming the suitability of the TSD model. The environmental conditions during the measurements and the specific phase of the cell cycle at the time of irradiation significantly impact the measurements and, consequently, the resulting survival curve [25]. The measurements employed in this study are derived from bibliographic sources; hence, these parameters are not emphasized.

TABLE IV
PARAMETERS OF THE TSD MODEL FOR THE THREE MICROORGANISMS.

Microorganism	MMSE	f_1	k_1	f_2	k_2
<i>Escherichia coli</i> O157.H71	0.0032	47.2702	1.1317	-9.1698	-0.0245
<i>Salmonella</i> spp.	0.0028	15.6008	0.4940	-9.1255	-0.0145
<i>Shigella dysenteriae</i> ATCC29027	0.0084	7.4598	0.4342	-7.8082	-0.1233

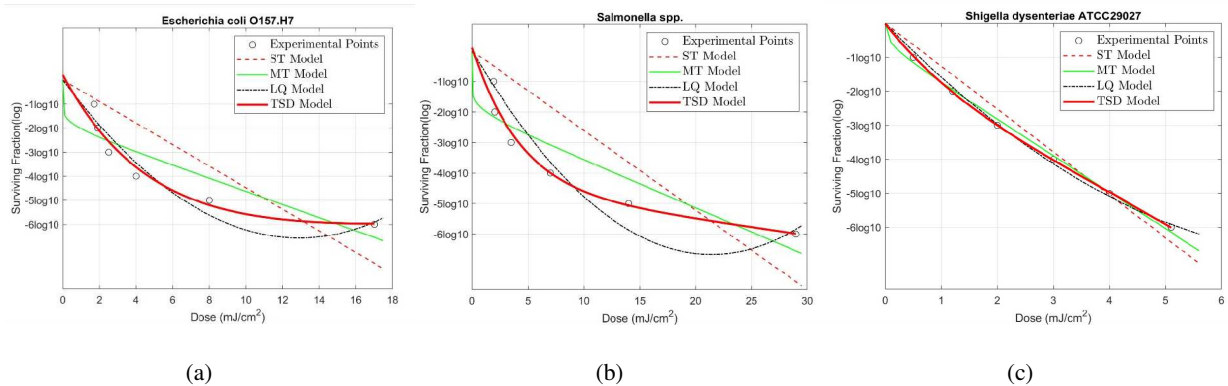


Fig. 3. Survival models for the three microorganisms in Table IV, with the TSD model offering the best fit.

VI. DISCUSSION

This study aimed to determine and parameterize the optimal survival curves for 33 fundamental microorganisms under UVC exposure through experimental measurements. By analyzing published data on UVC doses and corresponding survival fractions, we estimated parameters for four widely used survival models: the ST, MT, LQ, and TSD. We identified the best-fitting model for each microorganism by selecting the one with the minimum MSE relative to the experimental data.

Our findings indicate that the MT model was the most frequently suitable, accurately representing 21 of the 33 microorganisms studied. The TSD model was the best fit for three microorganisms but was unsuitable for the remaining ones. While the LQ model sometimes provided a good fit at lower doses, it was often discarded due to its unreliable behavior at higher doses. In conclusion, the evaluated models, particularly the MT model, offer robust predictive capabilities for the surface sterilization of microorganisms using UVC light. However, caution is advised when using the LQ model at higher doses due to its potential inaccuracies.

Employing the presented models for surface disinfection facilitates the prediction of the surviving fraction of each microorganism based on the administered UVC dose. These models can be integrated into simulators to achieve a realistic visualization of decontamination in three-dimensional space. One such simulator, LaUV, represents a state-of-the-art tool designed to investigate disinfection processes. LaUV precisely determines the trajectory of photons in three-dimensional space, accounting for their reflections on surfaces, scattering by air molecules, and ultimate absorption [27].

The simulator also enables the analysis of various factors that may influence sterilization, such

as the specific placement of UVC doses within a room and the varying albedo or roughness of different materials. Consequently, such an approach permits a more realistic and comprehensive disinfection study.

REFERENCES

- [1] A. Vavoulas, H. G. Sandalidis, N. D. Chatzidiamantis, Z. Xu, and G. K. Karagiannidis, "A survey on ultraviolet C-band (UV-C) communications," *IEEE Commun. Surveys Tuts.*, vol. 21, no. 3, pp. 2111–2133, 3rd Quart. 2019.
- [2] J. Turner and A. V. Parisi, "Ultraviolet radiation albedo and reflectance in review: The influence to ultraviolet exposure in occupational settings," *Int. J. Environ. Res. Public Health.*, vol. 15, no. 7, pp. 1507–1527, 2018.
- [3] W. Kowalski, *Ultraviolet Germicidal Irradiation Handbook*. New York, NY, USA: Springer-Verlag, 2010.
- [4] J. Lelieveld, F. Helleis, S. Borrmann, Y. Cheng, F. Drewnick, G. Haug, T. Klimach, J. Sciare, H. Su, and U. Pöschl, "Model calculations of aerosol transmission and infection risk of COVID-19 in indoor environments," *Int. J. Environ. Res. Public Health.*, vol. 17, no. 21, 2020, Art. no. 8114.
- [5] N. Demeersseman, V. Saegeman, V. Cossey, H. Devriese, and A. Schuermans, "Shedding a light on ultraviolet-c technologies in the hospital environment," *J. Hosp. Infect.*, vol. 132, pp. 85–92, 2023.
- [6] B. Wang, R. Mortazavi, and F. Haghghi, "Evaluation of modeling and measurement techniques of ultraviolet germicidal irradiation effectiveness - towards the design of immune buildings," *Indoor Built Environ.*, vol. 18, no. 2, pp. 101–112, 2009.
- [7] M. Raeiszadeh and B. Adeli, "A critical review on ultraviolet disinfection systems against COVID-19 outbreak: Applicability, validation, and safety considerations," *ACS Photonics*, vol. 7, no. 11, pp. 2941–2951, 2020.
- [8] P. Arguelles, "Estimating UV-C sterilization dosage for COVID-19 pandemic mitigation efforts," 2020, preprint, April.
- [9] R. Bhardwaj and A. Agrawal, "How coronavirus survives for days on surfaces," *Phys. Fluids*, vol. 32, no. 11, 2020.
- [10] P. Vasickova, I. Pavlik, M. Verani, and A. Carducci, "Issues concerning survival of viruses on surfaces," *Food Environ. Virol.*, vol. 2, no. 1, pp. 24–34, 2010.
- [11] M. Lindblad, E. Tano, C. Lindahl, and F. Huss, "Ultraviolet-c decontamination of a hospital room: Amount of UV light needed," *Burns*, vol. 46, no. 4, pp. 842–849, 2020.
- [12] S. B. Botta, F. de Sá Teixeira, F. S. Hanashiro, W. W. de Araújo, A. Cassoni, and M. C. B. da Silveira Salvadori, "Ultraviolet-c decontamination of a dental clinic setting: Required amount of UV light," *Braz. Dent. Sci.*, vol. 23, no. 2, 2020.
- [13] C. H. Thatcher and B. R. Adams, "Modeling specular and diffuse reflection of UV leds for microbial inactivation in air ducts," *Chem. Eng. Sci.*, vol. 263, 2022, Art. no. 118105.
- [14] Y. Cao, W. Chen, M. Li, B. Xu, J. Fan, and G. Zhang, "Simulation based design of deep ultraviolet LED array module used in virus disinfection," in *2020 21st Int. Conf. on Electron. Packag. Technol. (IEEE ICEPT)*, Guangzhou, China, Aug. 2020.
- [15] A. Baluja, J. Arines, R. Vilanova, J. Cortiñas, C. Bao-Varela, and M. T. Flores-Arias, "UV light dosage distribution over irregular respirator surfaces: Methods and implications for safety," *J. Occup. Environ. Hyg.*, vol. 17, no. 9, pp. 390–397, 2020.
- [16] B. Ngom, M. Thiam, M. F. Mbaye, M. Sow, K. Hann, and M. Wade, "Design and realization of a UV-C based disinfection tool monitored by mobile application," *Open J. Appl. Sci.*, vol. 12, no. 01, pp. 155–163, 2022.

- [17] K. Narita, K. Asano, K. Naito, H. Ohashi, M. Sasaki, Y. Morimoto, T. Igarashi, and A. Nakane, "Ultraviolet c light with wavelength of 222 nm inactivates a wide spectrum of microbial pathogens," *J. Hosp. Infect.*, vol. 105, no. 3, pp. 459–467, 2020.
- [18] M. Buonanno, D. Welch, I. Shuryak, and D. J. Brenner, "Far-UVC light (222 nm) efficiently and safely inactivates airborne human coronaviruses," *Sci. Rep.*, vol. 10, 2020, Art. no. 10285.
- [19] F. Chiappa, B. Frascella, G. P. Vigezzi, M. Moro, L. Diamanti, L. Gentile, P. Lago, N. Clementi, C. Signorelli, N. Mancini, and A. Odone, "The efficacy of ultraviolet light-emitting technology against coronaviruses: A systematic review," *J. Hosp. Infect.*, vol. 114, pp. 63–78, 2021.
- [20] M. Heßling, K. Hönes, P. Vatter, and C. Lingenfelder, "Ultraviolet irradiation doses for coronavirus inactivation—review and analysis of coronavirus photoinactivation studies," *GMS Hyg. Infect. Control*, vol. 15, 2020.
- [21] Wikipedia, "Log reduction," online; Accessed: 2025-04-23. [Online]. Available: https://en.wikipedia.org/wiki/Log_reduction/
- [22] M. E. R. Darnell, K. Subbarao, S. M. Feinstone, and D. R. Taylor, "Inactivation of the coronavirus that induces severe acute respiratory syndrome, sars-cov," *J. Virol. Methods*, vol. 121, no. 1, pp. 85–91, 2004.
- [23] J. L. Sagripanti and C. D. Lytle, "Sensitivity to ultraviolet radiation of lassa, vaccinia, and ebola viruses dried on surfaces," *Arch. Virol.*, vol. 156, pp. 489–494, 2011.
- [24] Radiology Key, "Cell survival curves," online; Accessed: 2025-04-23. [Online]. Available: <https://radiologykey.com/5-cell-survival-curves/>
- [25] S. J. McMahon, "The linear quadratic model: Usage, interpretation and challenges," *Phys. Med. Biol.*, vol. 64, no. 1, 2018, Art. no. 01TR01.
- [26] T. Nomiya, "Discussions on target theory: Past and present," *J. Radiat. Res.*, vol. 54, no. 6, pp. 1161–1163, 2013.
- [27] M. S. Baltadourou, K. K. Delibasis, G. N. Tsigaridas, H. G. Sandalidis, and G. K. Karagiannidis, "LaUV: A physics-based UV light simulator for disinfection and communication applications," *IEEE Access*, vol. 9, pp. 137 543–137 559, 2021.